

mTORC1 restrains adipocyte lipolysis to prevent systemic hyperlipidemia



Lauren M. Paoella^{1,2,3}, Sarmistha Mukherjee^{1,3}, Cassie M. Tran^{1,3}, Bruna Bellaver^{3,4}, Mindy Hugo^{1,2}, Timothy S. Luongo^{1,3}, Swapnil V. Shewale⁵, Wenyun Lu⁶, Karthikeyani Chellappa^{1,3}, Joseph A. Baur^{1,2,3,*}

ABSTRACT

Objective: Pharmacological agents targeting the mTOR complexes are used clinically as immunosuppressants and anticancer agents and can extend the lifespan of model organisms. An undesirable side effect of these drugs is hyperlipidemia. Although multiple roles have been described for mTOR complex 1 (mTORC1) in lipid metabolism, the etiology of hyperlipidemia remains incompletely understood. The objective of this study was to determine the influence of adipocyte mTORC1 signaling in systemic lipid homeostasis *in vivo*.

Methods: We characterized systemic lipid metabolism in mice lacking the mTORC1 subunit Raptor (Raptor^{ΔKO}), the key lipolytic enzyme ATGL (ATGL^{ΔKO}), or both (ATGL-Raptor^{ΔKO}) in their adipocytes.

Results: Mice lacking mTORC1 activity in their adipocytes failed to completely suppress lipolysis in the fed state and displayed prominent hypertriglyceridemia and hypercholesterolemia. Blocking lipolysis in their adipose tissue restored normal levels of triglycerides and cholesterol in the fed state as well as the ability to clear triglycerides in an oral fat tolerance test.

Conclusions: Unsuppressed adipose lipolysis in the fed state interferes with triglyceride clearance and contributes to hyperlipidemia. Adipose tissue mTORC1 activity is necessary for appropriate suppression of lipolysis and for the maintenance of systemic lipid homeostasis.

© 2019 The Authors. Published by Elsevier GmbH. This is an open access article under the CC BY-NC-ND license (<http://creativecommons.org/licenses/by-nc-nd/4.0/>).

Keywords mTORC1; Adipose tissue; Lipolysis; Triglycerides; Rapamycin

1. INTRODUCTION

Therapeutic inhibition of mechanistic Target Of Rapamycin (mTOR) is important for immunosuppression and the treatment of certain cancers [1]. Recent interest in this pathway has been heightened by the demonstration that the prototypical mTOR inhibitor, rapamycin, extends the lifespan of model organisms from yeast to rodents [2–4]. However, these studies have also served to highlight our incomplete understanding of the mechanisms by which mTOR signaling influences physiology in different cell types and the etiology of the undesirable side effects that can accompany mTOR inhibition, which include an increased risk of new-onset diabetes and dyslipidemia, a major risk factor for cardiovascular diseases [5,6].

mTOR is a serine/threonine protein kinase that nucleates two structurally and functionally distinct complexes, mTORC1 (characterized by the presence of Raptor) and mTORC2 (characterized by the presence of Rictor) [1]. mTORC1 is the canonical target of rapamycin and is acutely inhibited by the drug, whereas mTORC2 is only disrupted after chronic rapamycin treatment in specific cell types and *in vivo* due to sequestration of the catalytic mTOR subunit [7–9]. mTORC1 is regulated by anabolic signals and amino acid availability to suppress

autophagy and promote protein, lipid, and nucleic acid synthesis as well as nutrient transport [10]. mTORC2 plays key roles in metabolism, cell survival, and proliferation through multiple mechanisms including regulation of the insulin/IGF1 signaling cascade via phosphorylation of AKT at S473 [10]. Targeted disruption of mTORC1 or mTORC2 has revealed that each complex has distinct and tissue-specific effects on signaling and metabolism [10].

Genetic or pharmacological targeting of the mTOR complexes has been shown to influence pathways that are important for whole body lipid homeostasis *in vivo*. These include changes in the expression of hepatic genes involved in lipogenesis and triglyceride (TG) secretion, suppression of lipoprotein lipase (LPL) activity, and overactivation of lipolysis via increased ATGL expression or PKA activity in adipocytes [11–18]. However, the relative importance of these pathways and how they interact remain unclear. Indeed, an increase in circulating TG after mTOR inhibition is somewhat paradoxical, given that mTORC1 promotes lipogenesis, and genetic ablation of either mTOR complex in the liver results in unaltered or decreased plasma lipids rather than an increase [17,19,20]. In cultured adipocytes, mTORC1 inhibition decreases *de novo* lipogenesis and increases lipolysis, the latter proposed to be via either upregulation of ATGL expression or increased

¹Department of Physiology, Perelman School of Medicine, University of Pennsylvania, Philadelphia, PA, 19104, USA ²Biochemistry and Molecular Biophysics Graduate Group, Perelman School of Medicine, University of Pennsylvania, Philadelphia, PA, 19104, USA ³Institute for Diabetes, Obesity, and Metabolism, Perelman School of Medicine, University of Pennsylvania, Philadelphia, PA, 19104, USA ⁴Programa de Pós-graduação em Ciência Biológicas-Bioquímica, Departamento de Bioquímica, Universidade Federal do Rio Grande do Sul, Porto Alegre, RS, Brazil ⁵Penn Cardiovascular Institute, Perelman School of Medicine, University of Pennsylvania, Philadelphia, PA, 19104, USA ⁶Lewis-Sigler Institute for Integrative Genomics, Department of Chemistry, Princeton University, Princeton, NJ, 08544, USA

*Corresponding author. Institute for Diabetes, Obesity, and Metabolism, Perelman School of Medicine, University of Pennsylvania, 12-114 Smilow Center for Translational Research, 3400 Civic Center Boulevard, Philadelphia, PA, 19104, USA. E-mail: baur@penmedicine.upenn.edu (J.A. Baur).

Received August 27, 2019 • Revision received November 20, 2019 • Accepted December 2, 2019 • Available online 13 December 2019

<https://doi.org/10.1016/j.molmet.2019.12.003>

PKA-dependent phosphorylation of HSL [11,15,21]. After rapamycin treatment, the effects on lipolysis have been less clear, with increased circulating non-esterified fatty acids (NEFA) reported in some studies and decreased NEFA in others [13,22–25]. Decreased expression and activity of lipoprotein lipase have been more consistently observed after rapamycin treatment *in vivo* [6,12,18,22,26]. Genetic ablation of adipocyte mTORC1 with AP2-Cre resulted in lean mice that were protected from hypercholesterolemia [27]. However, this Cre can have off-target and mosaic effects [28]. We and others have since generated a mouse model lacking Raptor specifically in adipocytes using adiponectin-Cre and reported increased [29] or unchanged NEFA [30]. Lee et al. further described progressive lipodystrophy with increased *de novo* lipogenesis in adipocytes and upward trends but no significant changes in cholesterol and TG [30]. In sum, the available data do not identify a clear or consistent role for adipocyte mTORC1 signaling in systemic lipid homeostasis, and prior studies have been somewhat confounded by concurrent lipodystrophy.

Herein we studied mice with adipose-specific Raptor ablation (Raptor^{AKO}) prior to the onset of lipodystrophy. We show that these animals displayed profound hypertriglyceridemia specifically in the fed state. Although lipoprotein lipase expression decreased, the effect size was small, and this change alone did not explain the lipidomic profile in adipose tissue, which favored the accumulation of di- and mono-acylglycerols. While Raptor^{AKO} mice had lower NEFA than controls during fasting, they had higher NEFA in the fed state, suggesting a failure to appropriately suppress lipolysis and potentially explaining why *in vivo* studies on rapamycin have reached opposite conclusions with respect to its effects on circulating NEFA. Strikingly, genetic ablation of ATGL to limit adipocyte lipolysis largely restored triglyceride homeostasis without correcting the deficiency in lipoprotein lipase expression. These results suggest that unrestrained lipolysis is the primary defect in hyperlipidemia induced by adipocyte mTORC1 inhibition *in vivo*.

2. MATERIALS AND METHODS

2.1. Animals and treatments

All experiments were approved by the Institutional Animal Care and Use Committee at the University of Pennsylvania. Adipocyte-specific Raptor knockout mice (Raptor^{AKO}) were generated by crossing Raptor floxed mice containing loxP sites flanking exon 6 of the targeted *Rptor* (B6.Cg-Rptor^{tm1.1Dmsa/J}) with mice containing the Adipoq-Cre BAC transgene expressing Cre recombinase under the control of mouse adiponectin (Adipoq) promoter/enhancer regions (B6.FVB-Tg(Adipoq-Cre)1Evdrl/J) [31,32]. ATGL-Raptor^{AKO} mice were generated by crossing ATGL^{fl/fl} mice containing loxP sites flanking exons 2–7 of the *Pnpla2* gene (B6N.129S-Pnpla2^{tm1Eek/J}) [33]. with Raptor^{AKO} mice. The following primer sequences were used for genotyping: *Rptor*: forward, 5'-CTCAGTAGTGGTATGTGCTCAG-3'; reverse, 5'-GGGTA-CAGTATGTC AGCACAG-3'. *Pnpla2*: forward 5'-GAGTGCAGTGTCCCT-ACCA-3'; reverse 5'-ATCAGGCAGCCACTCCAAC-3'. Adipoq-Cre: forward 5'-ACCTCCTGGGAGAGTGAGGGC-3'; reverse 5'-GCATC-GACCGGTAATGCAGGC-3'. Age-matched floxed mice (Raptor^{fl/fl}, Raptor^{fl/fl}, ATGL^{fl/fl}, ATGL^{fl/fl}), Raptor^{AKO}, ATGL^{AKO}, and ATGL-Raptor^{AKO} male mice were studied between 10 weeks and 12 weeks of age unless otherwise stated. For fasting and refeeding experiments, the mice were fasted overnight and refed for 4 h. To stimulate lipolysis, the mice were injected intraperitoneally with 1 mg/kg β 3-adrenergic receptor agonist, CL316,243 (Sigma—Aldrich). For rapamycin treatment, the mice were intraperitoneally injected with 2 mg/kg rapamycin (LC

Laboratories) in 0.25% PEG400/Tween80 daily for 2 weeks. To suppress lipolysis, the mice were intraperitoneally injected with 100 mg/kg GPR81 Agonist, 3CI–5OH-BA (Sigma—Aldrich), at the beginning of refeeding. The mice were sacrificed by cervical dislocation after an overnight fast and 4 h of refeeding.

2.2. Western blotting analysis

Tissue samples were lysed in RIPA buffer supplemented with 10 μ L/mL Halt Protease and Phosphatase Inhibitor Cocktail (Thermo Fisher Scientific, 78440) and homogenized using TissueLyser II (Qiagen). The lysates were incubated with gentle rocking for 30 min at 4 °C and then centrifuged at 12,000 g for 20 min at 4 °C twice, transferring the supernatant. The protein concentration was determined via a BCA Assay (Pierce). Overall, 12–20 μ g of total protein was loaded onto sodium dodecyl sulfate-polyacrylamide gel electrophoresis (SDS-PAGE) 4–15% Tris-Glycine gradient gels or 10% resolving gels (Bio-Rad) and subsequently transferred to PVDF membranes (Bio-Rad). The membranes were blocked with either 3% BSA (for phospho-proteins) or 3% non-fat dry milk in TBST (50 mM Tris, pH 7.6, 150 mM NaCl, 0.1% tween 20) and incubated overnight at 4 °C in blocking solution with the following primary antibodies at 1:2000: Raptor (Cell Signaling, 2280), ATGL (Cell Signaling, 2138), pAkt Ser-473 (Cell Signaling, 9271), Akt (Cell Signaling, 9272), pS6 Ser240/Ser244 (Cell Signaling, 2215), S6 (Cell Signaling, 2212), p4EBP1 Ser-65 (Cell Signaling, 9451), and 4EBP1 (Cell Signaling, 9452). Secondary HRP conjugated antibodies (Jackson ImmunoResearch Laboratories, Inc.) were used at 1:10,000 in TBST and 1:10,000 for HRP conjugated B-actin (Abcam, 9620272). Immunolabeling was detected using PICO Plus or Femto ECL reagent (Pierce). Band densities were quantified using Image Lab version 5.2.1 and were normalized to β -actin (Bio-Rad).

2.3. Plasma lipid analysis

Blood was collected from the tail veins of the mice in Microvette CB300 LH K2E tubes (Sarstedt). For retro-orbital bleeding, mice were first anesthetized with isoflurane. Blood was collected to Fisherbrand Micro Blood Collecting Tubes, Natelson. Plasma was analyzed for cholesterol using Infinity Cholesterol Liquid Stable Reagent (Thermo Fisher Scientific, TR13421), triglycerides using Infinity Triglycerides Liquid Stable Reagent (Thermo Fisher Scientific, TR22421), non-esterified fatty acids using a Free Fatty Acid Kit (Wako, HR series NEFA-HR(2)), and glycerol using Free Glycerol Reagent (Sigma, F6428) according to the manufacturer's instructions.

2.4. Tissue triglycerides

Tissue pieces were homogenized in a 20x volume of 2:1 chloroform:methanol and then incubated at room temperature with agitation for 3 h. After the addition of 0.9% NaCl, the samples were vortexed and centrifuged (2000 rpm, 10 min). The organic phase was collected and dried under N₂ gas. The TG content was measured using the Infinity Triglycerides Liquid Stable Reagent (Thermo Fisher Scientific, TR22421) and normalized to the starting tissue weight.

2.5. Hepatic TG secretion

The mice were either fasted for 4 h or overnight and refed for 4 h and injected intraperitoneally with 1 g/kg body weight Pluronic F-127 (P-407) (BASF, 30085239) in PBS. Blood was drawn at indicated time points after P-407 injection. A total of 2 mL/kg of blood was collected at each time point. Plasma triglycerides and NEFA were measured. For CL316,243 treatment, the mice were injected 1 h post-P-407 injection.

2.6. Oral fat tolerance test

The mice were fasted overnight and fed 2 mg/g body weight of olive oil (Acros, 8001-25-0) through oral gavages. Approximately 50 μ L of blood was collected at baseline (prior to gavage) and at indicated time points. Plasma triglycerides and NEFA were measured. For CL316,243 treatment, the mice were injected 1 h post-gavage.

2.7. Quantitative real-time RT-PCR analysis

Total RNA was extracted using TRIzol. RNA was used to generate cDNA with a High Capacity Reverse Transcription Kit (Applied Biosystems). Reactions were run on a 7900 HT Fast Real-Time PCR System (Applied Biosystems) using SYBR Green Master Mix (Applied Biosystems) with the results normalized to *Tbp*. The primer sequences are listed in [Supplementary Table 1](#).

2.8. Post-heparin plasma LPL

Mice were either fasted for 4 h or overnight and refed for 4 h then injected with 0.5 units/g body weight (4 μ L/g of 125 units/ml in sterile PBS) of heparin (Sagent, 25021-400-10) through their tail vein. The mice were bled retro-orbitally at baseline and then 10 min after heparin injection. Plasma LPL activity was assayed using a Lipoprotein Lipase (LPL) Activity Assay Kit (Fluorometric) (Cell Biolabs, STA-610) according to the manufacturer's instructions.

2.9. Tissue LPL activity

Tissues (IWAT, EWAT, BAT, and skeletal muscle) were assayed using a Lipoprotein Lipase (LPL) Activity Assay Kit (Fluorometric) (Cell Biolabs, STA-610) according to the manufacturer's instructions.

2.10. Lipidomics

Liquid chromatography mass spectrometry (LC-MS) analysis of the lipids from the mice adipose samples was performed as follows. Approximately 30 mg of frozen tissue samples were weighed and then pulverized in a CryoMill (Retsch, Haan, Germany) with a stainless ball at liquid nitrogen temperature. Then, 1 mL of 0.1 M HCl in 50:50 methanol:H₂O was added to the tissue powder, vortexed for 10 s, and let sit at -20°C for 30 min. Next, 0.5 mL of chloroform was added to the mixture, vortexed to mix well, and let sit on ice for 10 min. The samples were centrifuged at 13,200 rpm for 10 min and the chloroform phase at the bottom was transferred to a glass vial using a Hamilton syringe as the first extract. Then 0.5 mL of chloroform was added to the remaining material and the extraction was repeated to obtain the second extract. The combined extract was dried under nitrogen flow and re-dissolved in solvent of 1:1:1 methanol:chloroform:2-propanol using a ratio of 1 mL of solvent per 10 mg of initial tissue weight. Fatty acids and lipids were analyzed on a Q Exactive Plus mass spectrometer coupled to a vanquish UHPLC system (Thermo Fisher Scientific, San Jose, CA, USA). Each sample was analyzed twice using the same LC gradient but different ionization modes on a mass spectrometer to cover both the positively charged and negatively charged species. The LC separation was achieved on an Agilent Poroshell 120 EC-C18 column (150 \times 2.1 mm, 2.7 μ m particle size) at a flow rate of 150 μ L/min. The gradient was 0 min, 25% B; 2 min, 25% B; 4 min, 65% B; 16 min, 100% B; 20 min, 100% B; 21 min, 25% B; and 27 min, 25% B [34]. Solvent A was 1 mM ammonium acetate +0.2% acetic acid in water:methanol (90:10). Solvent B was 1 mM ammonium acetate +0.2% acetic acid in methanol:2-propanol (2:98). For all experiments, 5 μ L of extract was injected with the column temperature set to 60°C . The Q-Exactive Plus mass spectrometer was operated at a scanning m/z of 70–1000 with a resolution (at m/z 200) of 140,000. The MS parameters were as follows: sheath gas flow

rate, 28 (arbitrary units); aux gas flow rate, 10 (arbitrary units); sweep gas flow rate, 1 (arbitrary units); spray voltage, 3.3 kV; capillary temperature, 320°C ; S-lens RF level, 65; AGC target, 3E6; and maximum injection time, 500 ms. Data analyses were performed using MAVEN software, which allows for sample alignment, feature extraction, and peak picking [35]. The Extracted ion chromatogram for each metabolite was manually examined to obtain its signal using a customized metabolite library.

2.11. Ex vivo lipolysis

Epididymal adipose tissue was isolated from the randomly fed mice. Each fat pad was cut into equal size pieces and placed in a 96-well plate containing 150 μ L of phenol-free DMEM media (Thermo Fisher Scientific, 21063) supplemented with 2% fatty acid free bovine serum albumin (BSA) (Sigma, A8806). For mTORC1 inhibition, 500 nM rapamycin was added to the media. For ATGL inhibition, 100 μ M of atglistatin (MedKoo, 510273) was added to the media. The tissue pieces were pre-incubated for 60 min. For basal lipolysis, the tissue pieces were incubated in new media for 60 min. For stimulated lipolysis, the tissue pieces were pretreated with 1 μ M CL316,243 for 30 min. To detect the release of NEFA, the tissue pieces were then placed in a new well with the same media for 60 min. The media were measured for NEFA and normalized to protein. To determine the protein concentration, each piece was incubated with 1 mL of chloroform for 60 min. The tissue was then transferred and lysed in 0.3 M of NaOH containing 0.1% sodium dodecyl sulfate (SDS) and incubated overnight at 65°C . The protein concentration was determined by a BCA assay.

2.12. Statistical analysis

All data are presented as mean \pm SEM and were analyzed using Prism version 8.2.0 (GraphPad). Statistical significance was determined using an unpaired two-tailed Student's *t*-test for single comparisons and one-way or two-way ANOVA followed by Tukey's post hoc test for multiple comparisons unless otherwise indicated.

3. RESULTS

3.1. Adipocyte-specific loss of mTORC1 activity elevates plasma lipids prior to lipodystrophy

To investigate the role of adipose mTORC1 on plasma lipid metabolism, we generated mice with adipose-specific deletion of Raptor (Raptor^{AKO}), which encodes an essential subunit of mTORC1. Deletion of Raptor in inguinal white adipose tissue (IWAT), epididymal white adipose tissue (EWAT), and brown adipose tissue (BAT), along with the expected reduction in phosphorylation of mTORC1 targets, ribosomal protein S6, and eukaryotic translation initiation factor 4E binding protein 1 (4EBP1) was confirmed by Western blotting ([Figure 1A,B](#), [Supplementary Figure 1A–C](#)). We also observed an increase in the phosphorylation of AKT as expected due to the loss of negative feedback on the insulin signaling cascade [36]. Deletion of Raptor did not change body weight in male ([Figure 1C](#)) or female mice ([Supplementary Figure 1D](#)), despite the onset of lipodystrophy by approximately 3 months of age, as reported previously [30]. We noted elevated expression of macrophage markers in EWAT ([Supplementary Figure 1F](#)), and the relative adipose mass decreased with age in both genders, while the liver mass increased ([Figure 1D](#), [Supplementary Figure 1E](#)). In contrast to the mild or protective lipid phenotypes observed in previous studies, we noted consistent hypertriglyceridemia in the Raptor^{AKO} mice ([Supplementary Figure 1G, H](#)). To avoid the confounding effects of decreased adipose tissue mass, we studied the

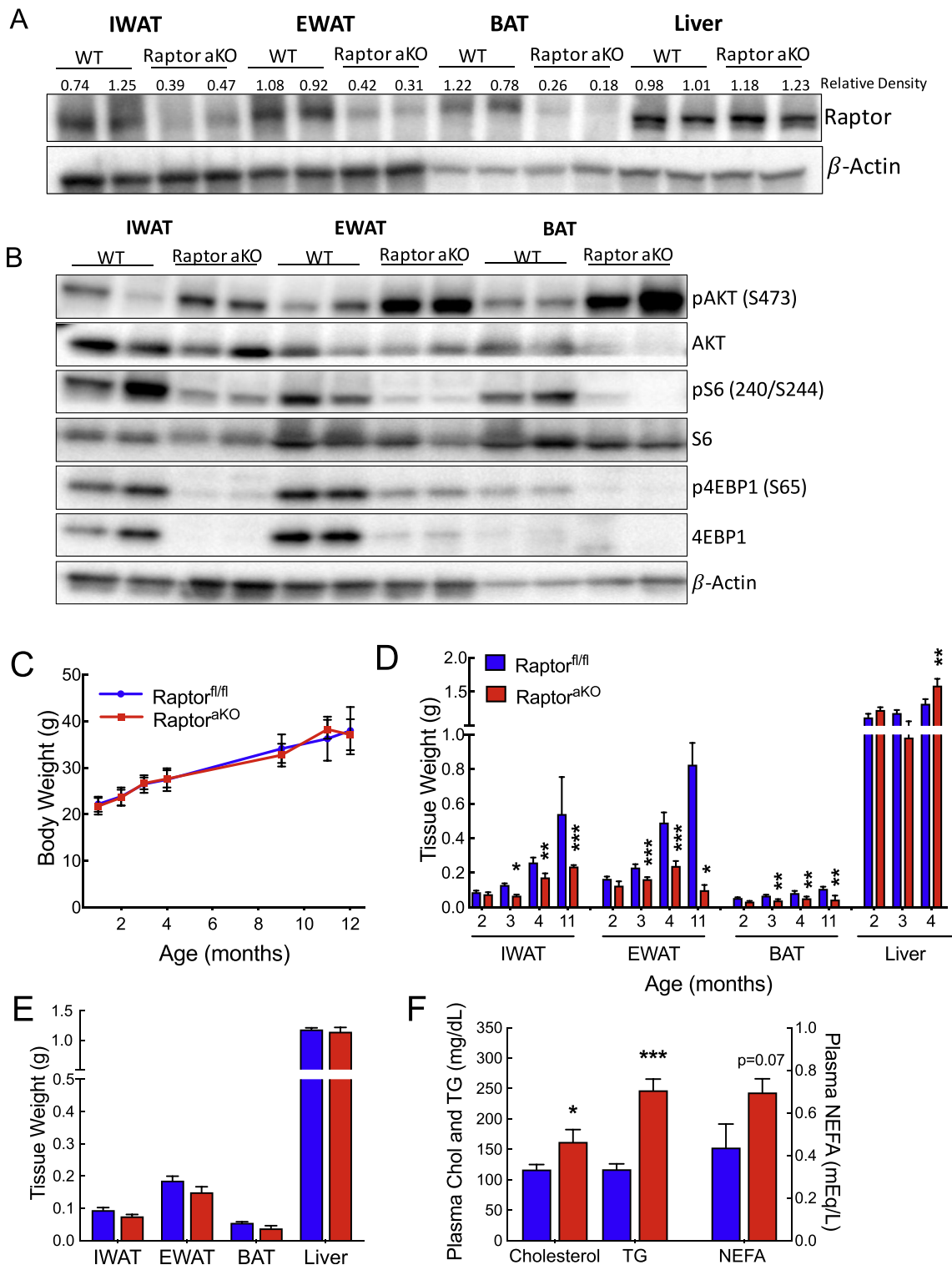


Figure 1: Adipocyte-specific ablation of mTORC1 elevates plasma lipids prior to lipodystrophy. (A) Western blotting for Raptor in IWAT, EWAT, BAT, and liver. Numbers indicate relative density normalized to β -actin. (B) Western blotting of downstream mTORC1 substrates in IWAT, EWAT, and BAT of Raptor^{aKO} and Raptor^{fl/fl} littermates. (C) Body and (D) tissue weights with age of male Raptor^{aKO} mice compared to controls (male, $n = 3-11$). (E) Tissue weights and (F) random fed plasma lipid parameters of 10-week-old Raptor^{aKO} mice ($n = 6-9$). Data presented as mean \pm s.e.m. * $p < 0.05$, ** $p < 0.01$, *** $p < 0.001$.

mice at ~10 weeks of age, a time point at which the sizes of adipose depots were similar between genotypes (Figure 1E). At this age, we also noted no evidence of hepatic steatosis (Supplementary Figure 1). We found that random fed plasma cholesterol and triglycerides were increased in the Raptor^{akO} mice as compared to those in the controls and that a trend toward increased non-esterified fatty acids (NEFA) was also apparent (Figure 1F). We conclude that the Raptor^{akO} mice developed hyperlipidemia prior to lipodystrophy.

3.2. Plasma lipid levels are sensitive to adipocyte mTORC1 status in the fed state

Hyperlipidemia has not been reported in previous studies of mice lacking adipocyte mTORC1 signaling, and reports conflict regarding the effect of pharmacologic mTORC1 inhibition on NEFA. To determine whether changes in the feeding state might explain these apparent contradictions, we subjected the mice to an overnight fast and subsequent 4 hour period of refeeding. We found that the effect of adipocyte mTORC1 ablation on circulating TG was entirely feeding state-dependent. In the fasted state, plasma TG were similar between the Raptor^{akO} mice and controls, whereas in the re-fed state, the Raptor^{akO} mice displayed profound elevations in their circulating TG (Figure 2A). Moreover, the Raptor^{akO} mice demonstrated significantly lower NEFA in the fasted state, when lipolysis is normally activated, but significantly higher NEFA in the fed state, when lipolysis would normally be repressed (Figure 2B). Compared to the controls, the Raptor^{akO} mice gained a similar amount of weight during refeeding and maintained similar blood glucose levels, suggesting that the altered lipid parameters were not due to changes in their food intake (Supplementary Figure 2). We hypothesized that higher NEFA in the fed state might lead to an increase in re-esterification to TG in the liver and secretion as VLDL particles, which could explain the elevation of plasma TG. However, the rate of hepatic TG secretion (assessed by blocking lipase activity with non-ionic surfactant P-407 and monitoring the rate of increase of plasma TG) was unchanged in the Raptor^{akO} mice in either the fasted or the fed state, despite higher levels of plasma TG before P-407 injection in the re-fed condition (Figure 2C). Next, we administered an oral fat tolerance test, which bypasses first-pass hepatic metabolism, to measure TG clearance. Consistent with an extrahepatic cause of hypertriglyceridemia, the Raptor^{akO} mice displayed increased plasma TG as compared to the controls (Figure 2D). This finding indicated a defect in the clearance of plasma TG in the Raptor^{akO} mice.

3.3. Adipocyte-specific ablation of mTORC1 activity causes a modest deficiency in lipoprotein lipase expression

To determine the cause of delayed clearance in the Raptor^{akO} mice, we examined lipoprotein lipase (LPL) gene expression and activity. LPL plays a central role in the clearance of lipid from plasma by hydrolyzing TG to NEFA and monoacylglycerols (MG). LPL protein translocates from the cell of origin to the luminal surface of endothelial cells, where it is bound by proteoglycans and can act on circulating lipoprotein particles. LPL is active in adipose tissue after feeding and can be released into the circulation by the administration of heparin. We found that *Lpl* gene expression decreased in the IWAT and EWAT from the Raptor^{akO} mice (Figure 3A). Consistent with a defect in adipocyte *Lpl* expression in the Raptor^{akO} mice, we observed a decrease in heparin-releasable LPL activity in the fed state, but not during fasting (Figure 3B). Direct assay of LPL activity extracted from tissue lysates revealed decreases in the IWAT and BAT of the re-fed Raptor^{akO} mice (Figure 3C). In contrast, we were unable to measure a defect in EWAT despite the reduction in *Lpl* mRNA level. Although the reason for this discrepancy was not clear, we

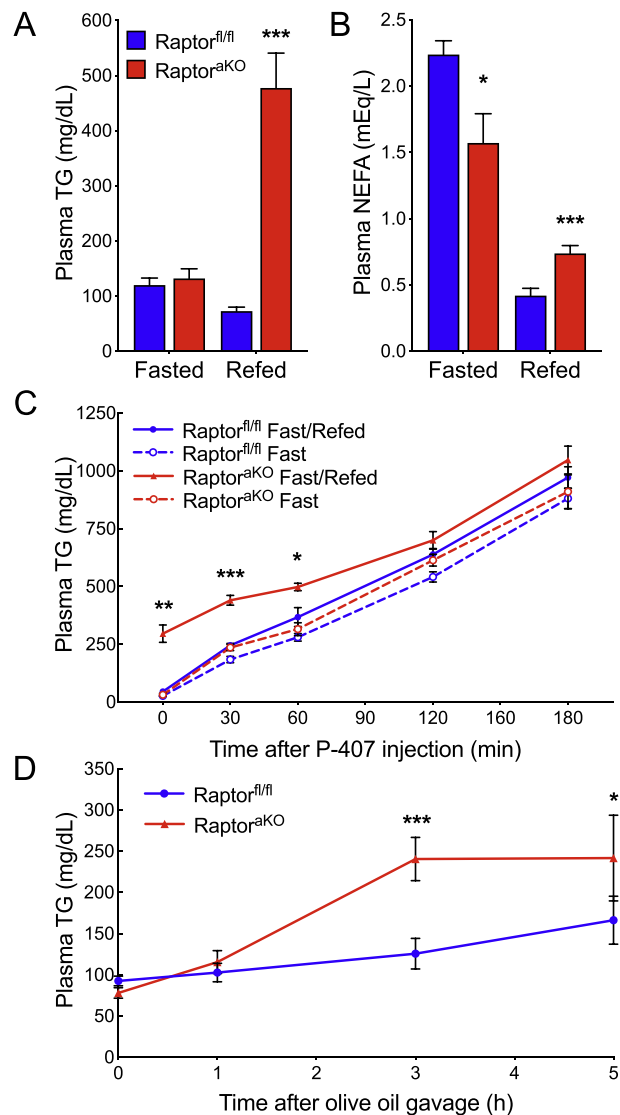


Figure 2: Adipocyte-specific ablation of mTORC1 elevates plasma lipids upon refeeding. Ten-week-old Raptor^{fl/fl} and Raptor^{akO} mice were fasted overnight and re-fed. (A) Plasma TG (n = 8–10). (B) Plasma NEFA (n = 8–10). (C) Mice were fasted (n = 5) or fasted and re-fed (n = 3–4) as described in the methods, and plasma TG was measured at indicated time points after injection with P-407 to measure hepatic TG secretion. (D) Mice were fasted and plasma TG was measured at indicated time points during an oral fat tolerance test to measure the clearance of circulation TG (n = 6–8). Data presented as mean ± s.e.m. *p < 0.05, **p < 0.01, ***p < 0.001.

speculate that reduced shedding of the LPL into the bloodstream may have helped maintain tissue levels in the Raptor^{akO} mice. Overall, decreases in the LPL activity were significant, but generally mild in the Raptor^{akO} mice. Thus, we tested whether other factors might also have contributed to the hyperlipidemia and lipodystrophy in the Raptor^{akO} animals.

3.4. Lipidomic profiling reveals accumulation of lipolytic intermediates in adipose-specific mTORC1 KO mice

To gain further insight into the alterations in adipocyte lipid metabolism that occur in the absence of mTORC1 signaling, we assayed lipidomic profiles in the adipose from the Raptor^{akO} mice and their wild-type

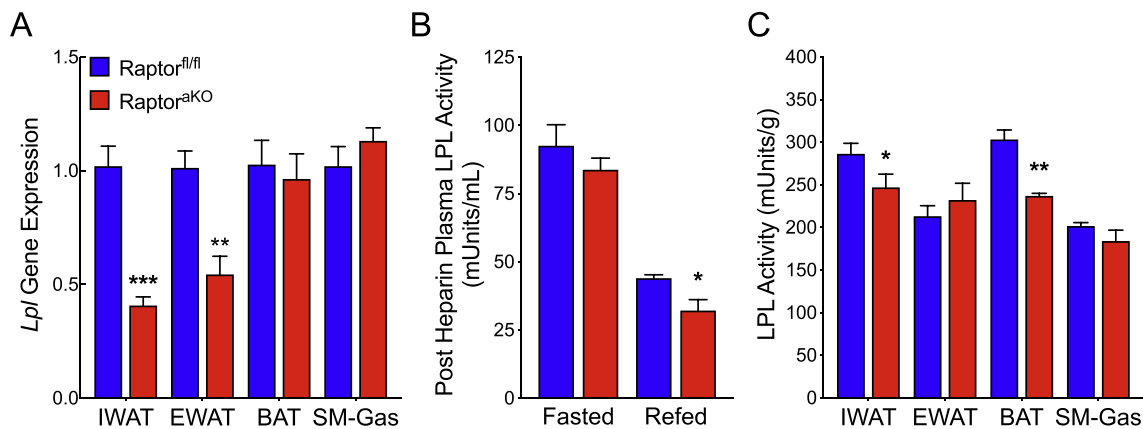


Figure 3: Adipocyte-specific ablation of mTORC1 causes a modest deficiency in lipoprotein lipase. (A) *Lpl* gene expression normalized to TBP for IWAT, EWAT, BAT, and skeletal muscle from re-fed 10-week-old Raptor^{fl/fl} and Raptor^{akO} mice ($n = 4-6$). (B) Post-heparin plasma LPL activity in the fasted and re-fed state ($n = 6$). (C) Tissue LPL activity for IWAT, EWAT, BAT, and skeletal muscle ($n = 4$). Data presented as mean \pm s.e.m. * $p < 0.05$, ** $p < 0.01$, *** $p < 0.001$.

littermates in the re-fed state at 10 weeks of age. Simple inhibition of LPL would be expected to decrease the abundance of NEFA, MG, and diacylglycerols (DG) in the adipose tissue, because fewer of these metabolites would be released from the circulating TG and available for re-esterification. In contrast, the lipidomic profiles revealed an increase in the abundance of MG and DG species and a decrease in the total TG content in the Raptor^{akO} adipose (Figure 4A–E). The relative abundances of each lipid species in the Raptor^{fl/fl} vs Raptor^{akO} mice are listed in Supplementary Table 2. The increases in MG and DG suggest that either re-esterification was impaired or lipolysis was activated. These possibilities could be distinguished because lipolysis results in the release of free glycerol, whereas LPL-dependent hydrolysis of TG leaves the glycerol moieties trapped as MG. We found that the Raptor^{akO} mice in the re-fed state exhibited elevated glycerol concentrations, demonstrating increased lipolysis as a driver of elevated NEFA in this model (Figure 4F).

3.5. Genetic inhibition of lipolysis ameliorates hyperlipidemia in adipose-specific mTORC1 KO mice

To limit lipolysis in the context of Raptor deletion, we concurrently deleted adipocyte triglyceride lipase (ATGL), which encodes the rate-limiting enzyme for hydrolysis of adipocyte TG during lipolysis (Figure 5A,B). The ATGL protein levels in the liver were not altered upon adipose-specific ATGL deletion (Supplementary Figure 3A). Although body weight was unchanged, IWAT, EWAT, and BAT weights were increased in both the ATGL^{akO} and ATGL-Raptor^{akO} mice (Supplementary Figure 3B, C). ATGL loss restored re-fed plasma NEFA to normal levels in the Raptor^{akO} mice *in vivo* (Figure 5C) and blocked the increase in basal lipolysis observed explants derived from the Raptor^{akO} EWAT (Figure 5D). ATGL loss also prevented the induction of lipolysis by CL316,243 in both genotypes. In addition to the expected effects on lipolysis, ATGL deletion prevented the increase in re-fed plasma TG levels in the Raptor^{akO} mice (Figure 5E). Plasma cholesterol was also restored to normal levels (Supplementary Figure 3D). To exclude potential consequences of chronic deletion in the genetic models, we tested the effects of acute inhibition of mTORC1 and ATGL on *ex vivo* lipolysis. Inhibition of mTORC1 with rapamycin increased basal lipolysis, and the addition of the ATGL inhibitor atlistatin was able to prevent an increase (Figure 5F). Notably, the ATGL-Raptor^{akO} mice did not have significantly altered *Angptl4* mRNA as compared to the controls and had the same

reductions in *Plin1* and *Lpl* mRNA that were observed in Raptor^{akO} mice (Supplementary Figure 3E, F). This suggests the possibility that unrestrained lipolysis, rather than a defect in LPL expression, was the primary cause of impaired lipid clearance in the Raptor^{akO} mice, consistent with the suggestion that LPL might be subject to feedback inhibition by NEFA and MG [37–39]. However, mice lacking adipocyte ATGL have decreased hepatic TG stores and lower plasma TG levels during fasting. Therefore, it could also be speculated that this decrease in fasting plasma TG might buffer the increase upon refeeding. To more directly test the ability of the ATGL-Raptor^{akO} mice to clear a fixed load of TG, we conducted an oral fat tolerance test. Concurrent loss of ATGL restored the ability of the Raptor^{akO} mice to clear exogenous TG, limiting the increase in plasma TG to that seen in their floxed littermates (Figure 5G). Although the starting TG levels were lower with the loss of ATGL, the rate of clearance and area under the curve were comparable to those of the wild-type mice (Figure 5H). Thus, unrestrained lipolysis impaired the clearance circulation of TG-rich lipoproteins in the Raptor^{akO} mice.

3.6. Stimulating lipolysis is sufficient to delay clearance of plasma TG in WT mice

Our results at this point demonstrated that lipolysis drives hyperlipidemia in the context of Raptor^{akO} mice, which had multiple alterations in their lipid-handling pathways. To determine whether increased lipolysis *per se* is sufficient to impair the clearance of TG in wild-type mice, we conducted an oral fat tolerance test with or without stimulation of lipolysis with the β_3 -adrenergic agonist CL316,243. CL316,243 injection substantially increased plasma NEFA, as expected (Figure 6A). In mice that received the CL316,243 injections, clearance of the exogenous TG was also dramatically slowed, resulting in hyperlipidemia (Figure 6B). In contrast, CL316,243 did not increase plasma NEFA or plasma TG in mice lacking ATGL (Supplementary Figure 4). We next measured hepatic TG secretion to test whether CL316,243 could slow the apparent TG clearance rate by enhancing hepatic re-esterification of NEFA and packaging into TG-rich lipoproteins. Contrary to this hypothesis, we found that when peripheral TG uptake was blocked by treatment with P-407, CL316,243 actually decreased the rate of hepatic TG secretion and lowered plasma TG (Figure 6C,D). These data indicate that CL316,243 increased plasma TG by delaying LPL-dependent clearance, rather than by increasing hepatic TG secretion.

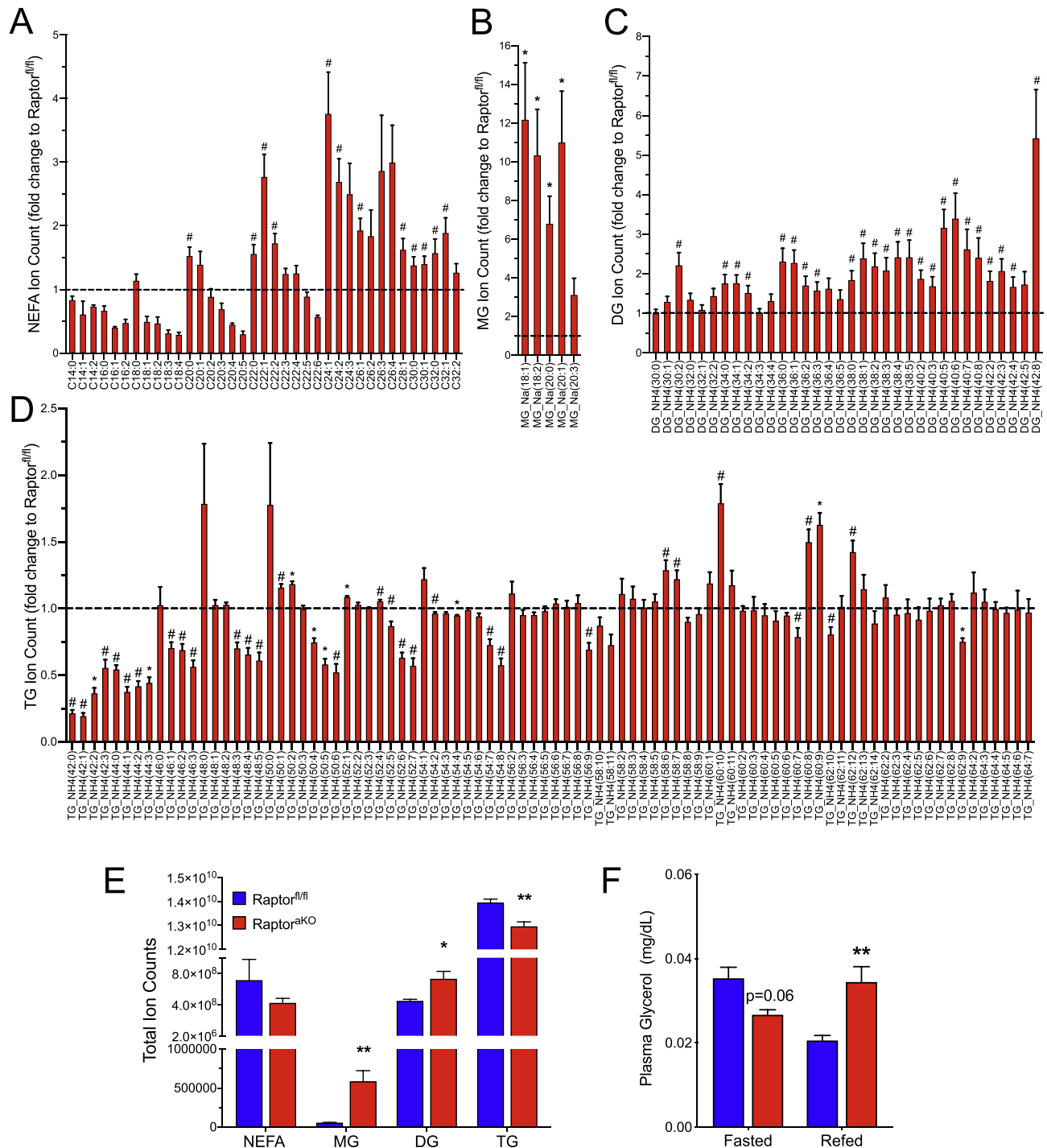


Figure 4: Adipocyte-specific ablation of mTORC1 alters intracellular lipids. Ten-week-old Raptor^{fl/fl} and Raptor^{akO} mice were fasted overnight and refed for 4 h prior to collection of EWAT for lipidomics. Fold change in relative abundance compared to Raptor^{fl/fl} for (A) NEFA, (B) monoacylglycerols (MG), (C) diacylglycerols (DG), and (D) triglycerides (TG) (n = 5–6). A–D: #p < 0.05 for two-tailed unpaired t-test prior to multiple comparisons and *p < 0.05 corrected for multiple comparisons using the Holm-Sidak method. (E) Total ion counts from (A–D). (F) Plasma glycerol (n = 3–6). Data presented as mean ± s.e.m. *p < 0.05, **p < 0.01, ***p < 0.001.

3.7. Inhibiting lipolysis restores plasma TG levels increased by rapamycin treatment

We next investigated whether inhibiting adipocyte lipolysis *in vivo* is sufficient to reverse rapamycin-induced hyperlipidemia. Wild-type mice were treated with rapamycin (2 mg/kg daily by intraperitoneal

injection) for 2 weeks to induce hypertriglyceridemia. To inhibit lipolysis selectively in their adipose tissue, we used a GPR81 agonist (3Cl–50H-BA). GPR81 is predominantly expressed in adipose tissue and physiological activation of this receptor by lactate leads to suppression of lipolysis [40,41]. This approach avoids inhibiting hepatic ATGL,

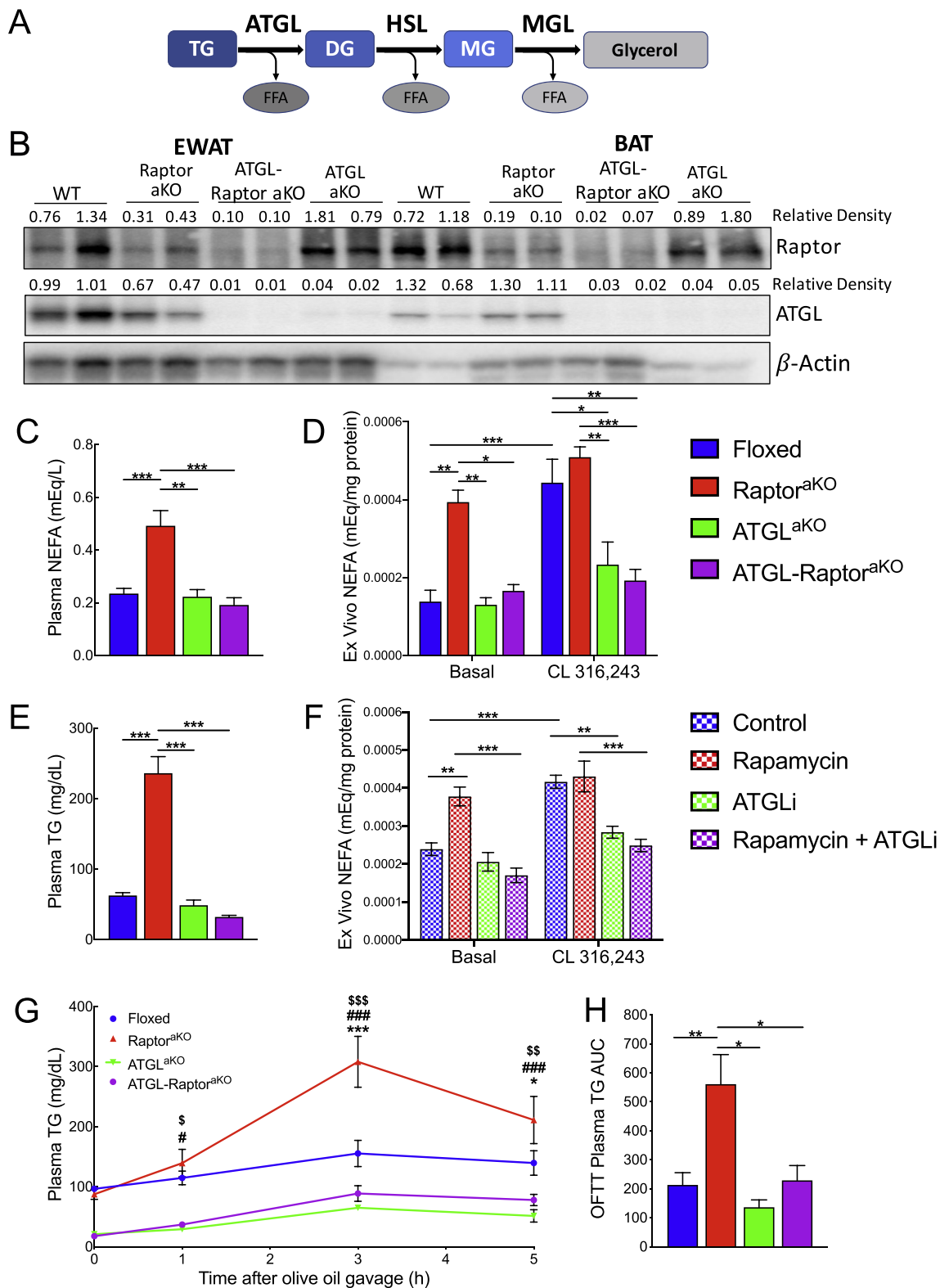


Figure 5: Genetic inhibition of lipolysis reverses lipid phenotypes of adipose-specific mTORC1 KO. Ten-week-old mice were fasted overnight and refed. (A) Diagram of the lipolysis pathway. (B) Western blotting and relative density (normalized to β -actin) of Raptor and ATGL protein from EWAT and BAT. (C) Refed plasma NEFA (floxed $n = 9$, Raptor^{aKO} $n = 5$, ATGL^{aKO} $n = 3$, and ATGL-Raptor^{aKO} $n = 9$). (D) Refed plasma TG (floxed $n = 9$, Raptor^{aKO} $n = 5$, ATGL^{aKO} $n = 3$, and ATGL-Raptor^{aKO} $n = 9$). (E) NEFA from *ex vivo* EWAT lipolysis with or without stimulation by 1 μ M CL316,243 (floxed $n = 10$, Raptor^{aKO} $n = 4$, ATGL^{aKO} $n = 5$, and ATGL-Raptor^{aKO} $n = 5$). (F) *Ex vivo* lipolysis in EWAT from wild-type mice treated with 500 nm rapamycin and 100 μ M atglistatin (G) Plasma TG clearance during an oral fat tolerance test and (H) AUC (floxed $n = 11$, Raptor^{aKO} $n = 12$, ATGL^{aKO} $n = 3$, and ATGL-Raptor^{aKO} $n = 11$). Data presented as mean \pm s.e.m. * = $p < 0.05$, ** = $p < 0.01$, *** = $p < 0.001$. (G) Raptor^{aKO} compared to floxed, * = $p < 0.05$, ** = $p < 0.01$, *** = $p < 0.001$. Raptor^{aKO} compared to ATGL-Raptor^{aKO} # = $p < 0.05$, ## = $p < 0.01$, ### = $p < 0.001$. Raptor^{aKO} compared to ATGL^{aKO} \$ = $p < 0.05$, \$\$ = $p < 0.01$, \$\$\$ = $p < 0.001$.

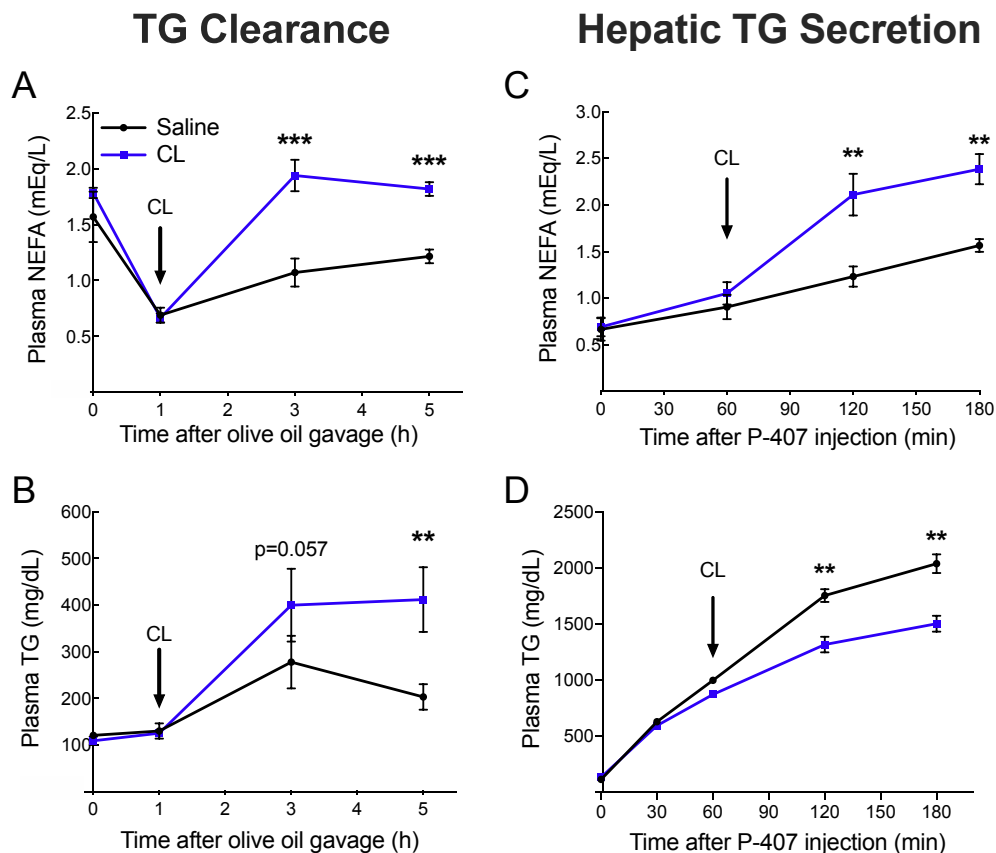


Figure 6: Increased plasma NEFA from lipolysis delays clearance of plasma TG. (A and B) Male C57BL/6 mice were fasted overnight and gavaged with olive oil for an oral fat tolerance test. Mice were injected with either saline or CL316,243 at 1 h (arrow). (A) Plasma NEFA and (B) plasma TG were measured at the indicated time points (n = 5–6). (C and D) Mice were fasted overnight and refed then injected with P-407 to measure hepatic TG secretion. Either saline or CL316,243 was injected at 1 h (arrow). (C) Plasma NEFA and (D) plasma TG was measured at indicated time points after P-407 injection. Data presented as mean \pm s.e.m. *p < 0.05, **p < 0.01, ***p < 0.001.

which complicates the interpretation of experiments pharmacologically targeting that enzyme. As expected, rapamycin-treated mice failed to fully suppress plasma NEFA levels upon refeeding, and this was corrected by treatment with the GPR81 agonist (Figure 7A). In parallel, the GPR81 agonist restored the refed plasma TG to control levels (Figure 7B). These results indicate that restoring adipocyte lipolysis to normal levels can mitigate rapamycin-induced hypertriglyceridemia.

4. DISCUSSION

Although mTORC1 is known to influence lipid metabolism through multiple pathways in multiple cell types, the precise etiology of hyperlipidemia induced by systemic mTORC1 inhibition *in vivo* remains uncertain. Indeed, genetic loss of mTORC1 in hepatocytes causes the opposite phenotype, lowering circulating cholesterol and TG [19,20]. Here, we show that loss of mTORC1 in adipocytes is sufficient to cause hypertriglyceridemia despite having only modest effects on the expression and *ex vivo* activity of lipoprotein lipase. Mechanistically, we show that although mTORC1 signaling affects many aspects of adipocyte biology, hypertriglyceridemia is driven primarily by unrestrained lipolysis in the fed state, which likely interferes with the *in situ* activity of lipoprotein lipase.

Studies of cultured adipocytes have demonstrated that inhibition of mTORC1 signaling with rapamycin leads to increased lipolysis in response to β -adrenergic stimulation via enhanced HSL phosphorylation [15], and more generally via activation of Egr1-dependent ATGL

transcription [11,21]. Here, we show that genetic deletion of ATGL in adipocytes is sufficient to normalize refed NEFA and TG levels in Raptor^{AKO} mice, supporting a model in which lipolysis drives hypertriglyceridemia. However, we did not observe a significant increase in ATGL protein expression in the adipose depots of the Raptor^{AKO} mice, consistent with several other studies [15,25,26,30]. This suggests that ATGL expression *per se* cannot account for the increase in lipolysis. A more general mechanism that can account for the widespread effects of Raptor deletion on lipid metabolism and might contribute to increased lipolysis is the suppression of PPAR γ and C/EBP α transcriptional activity in the absence of mTORC1 [22,30,42]. The phenotypes of adipose-specific C/EBP α KO mice are complicated by severe lipodystrophy early in life, but these animals exhibit impaired TG clearance [43]. Germline ablation of the C/EBP α target *Plin1* (encoding perilipin 1) mimics the lipolytic phenotype of Raptor^{AKO} mice; these animals have increased basal lipolysis and decreased stimulated lipolysis [44]. Moreover, decreased expression of *Plin1* is observed in mice treated with rapamycin [26] and in Raptor^{AKO} mice (Supplementary Figure 3F). Perilipin 1 coats the outside of lipid droplets to prevent hydrolysis by ATGL. Thus, a decrease in perilipin 1 expression is a mechanism that could account for an increase in ATGL-dependent lipolysis in the absence of a change in ATGL expression. Many prior studies have implicated decreased adipose LPL in the hypertriglyceridemia associated with rapamycin treatment [6,12,18,22,26]. Consistent with these reports, we observed a decrease in LPL gene expression and showed that TG clearance, but

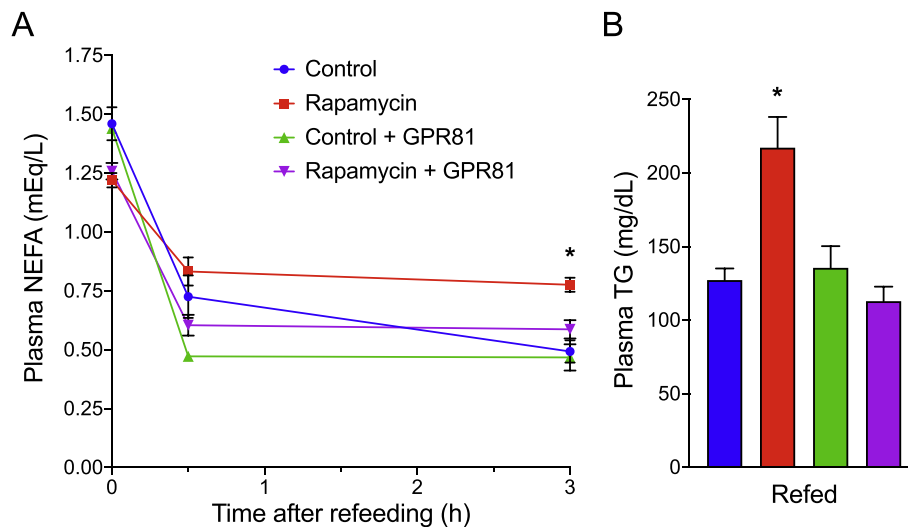


Figure 7: Inhibiting lipolysis restores plasma TG levels in rapamycin-treated mice. Male C57BL/6 mice were treated with 2 mg/kg rapamycin for 2 weeks to induce hyperlipidemia. Mice were fasted overnight and then injected with 100 mg/kg GPR81 agonist at the time of refeeding. (A) Plasma NEFA and (B) plasma TG were measured at 0, 0.5, and 3 h after refeeding. Data presented as mean \pm s.e.m. Compared to rapamycin treatment, * $p < 0.05$, ** $p < 0.01$, *** $p < 0.001$.

not hepatic production of TG-rich lipoproteins, was altered in the Raptor^{akO} mice. However, we were able to detect only small decreases in the LPL activity that could be released by heparin *in vivo* or extracted from adipose tissue. Moreover, deletion of ATGL restored TG clearance without correcting *Lpl* gene expression. LPL activity has been shown to be inhibited by *Angptl4*, *in vitro* and *in vivo*, which could account for differences in activity vs expression [45,46]. However, we were unable to detect consistent changes in *Angptl4* expression in the Raptor^{akO} mice, regardless of ATGL status (Supplementary Figure 3F). Another possibility to explain the disconnect between LPL expression and activity is inhibition due to local accumulation of NEFA and MG. It has long been demonstrated that NEFA can suppress LPL through multiple mechanisms, including product inhibition, displacement of the active enzyme from the endothelium, and preventing its interaction with activating factors such as ApoC-II [37,38,47,48]. As a “proof of principle” experiment for this mechanism, we stimulated adipose tissue lipolysis with a β -adrenergic agonist and showed that this was sufficient to delay TG clearance in an oral fat tolerance test. Similarly, a GPR81 agonist that suppresses adipocyte lipolysis was sufficient to acutely normalize plasma TG in the rapamycin-treated mice. Notably, acute dosing with niacin has been reported to suppress post-prandial hypertriglyceridemia in humans, and it was speculated that this might be related to a reduction in NEFA release from adipose [49,50]. Thus, we propose that inappropriate lipolysis in the fed state directly impairs LPL activity in the Raptor^{akO} mice, and that such inhibition may be a general feature of hyperlipidemia.

An interesting aspect of the elevated NEFA and TG phenotypes of Raptor^{akO} mice was their complete dependence on feeding status. This may explain conflicting reports on the effect of rapamycin on NEFA, which has been significantly increased in some studies and decreased in others [13,22–25]. It also clearly demonstrates that impaired adipocyte mTORC1 signaling is not the only factor contributing to rapamycin-induced hyperlipidemia, since circulating TG levels in rapamycin-treated animals are not completely resolved by fasting. In part, this may reflect the ability of rapamycin to reduce LPL expression in tissues such as skeletal and cardiac muscle that play a larger role in TG clearance during fasting. We also note that chronic rapamycin treatment can impair mTORC2 activity; as mice lacking mTORC2 in

adipose tissue have a defect in insulin-dependent suppression of lipolysis, both mTOR complexes may act together to fully restrain adipocyte lipolysis [51]. Consistent with a role of mTORC2 in rapamycin-induced hyperlipidemia, it was recently shown that a rapamycin derivative that avoids mTORC2 inhibition (DL001) also fails to induce hyperlipidemia in fasted mice [52]. The effect of DL001 on TG in fed mice has not been reported. Finally, although our data suggest that lipolysis can affect plasma cholesterol levels, it is unclear whether this is directly related to LPL activity. Further research is required to fully elucidate the mechanism and the degree to which loss of adipocyte mTORC1 recapitulates the hypercholesterolemic effects of rapamycin.

5. CONCLUSIONS

We demonstrated that mTORC1 signaling in adipose tissue is critical for the maintenance of plasma lipid homeostasis in the fed state. Lack of mTORC1 in adipocytes increases both lipolysis and circulating TG in fed mice. Lipolysis is causally related to hypertriglyceridemia, since genetic ablation of ATGL resolves both circulating NEFA and TG clearance rates. Moreover, direct stimulation of lipolysis in wild-type mice is sufficient to impair TG clearance. Thus, mTORC1-dependent suppression of adipocyte lipolysis is an essential switch to maintain plasma lipid concentrations during feeding.

AUTHOR CONTRIBUTIONS

LMP and JAB conceived the experiments, analyzed the data, and wrote the manuscript. LMP, CMT, SM, KC, BB, MH, WL, and TSL conducted the experiments. SM, KC, BB, SVS, and TSL helped edit and revise the manuscript.

ACKNOWLEDGMENTS

We thank the past and present members of the Baur Lab for their constructive feedback and suggestions. This study was supported by grants from the National Institutes of Health (AG043483 and DK098656 to JAB and F31AG057171 to LMP). BB was supported by Coordenação de Aperfeiçoamento de Pessoal de Nível Superior

(CAPES). We thank the members of the Rader Lab for their help with the protocols. We thank Paul Titchenell, Daniel Rader, and Joshua Rabinowitz (Princeton University) for helpful discussions. We thank the Penn Diabetes Research Center (DK19525) Metabolomics Core for the lipidomics analysis.

CONFLICT OF INTEREST

The authors declare no conflicts of interest.

APPENDIX A. SUPPLEMENTARY DATA

Supplementary data to this article can be found online at <https://doi.org/10.1016/j.molmet.2019.12.003>.

REFERENCES

- Benjamin, D., Colombi, M., Moroni, C., Hall, M.N., 2011. Rapamycin passes the torch: a new generation of mTOR inhibitors. *Nature Reviews Drug Discovery* 10(11):868–880.
- Harrison, D.E., Strong, R., Sharp, Z.D., Nelson, J.F., Astle, C.M., Flurkey, K., et al., 2009. Rapamycin fed late in life extends lifespan in genetically heterogeneous mice. *Nature* 460(7253):392–395.
- Miller, R.A., Harrison, D.E., Astle, C.M., Baur, J.A., Boyd, A.R., de Cabo, R., et al., 2011. Rapamycin, but not resveratrol or simvastatin, extends life span of genetically heterogeneous mice. *Journals of Gerontology Series A: Biological and Medical Sciences* 66(2):191–201.
- Medvedik, O., Lamming, D.W., Kim, K.D., Sinclair, D.A., 2007. MSN2 and MSN4 link calorie restriction and TOR to sirtuin-mediated lifespan extension in *Saccharomyces cerevisiae*. *PLoS Biology* 5(10):e261.
- Parekh, J., Corley, D.A., Feng, S., 2012. Diabetes, hypertension and hyperlipidemia: prevalence over time and impact on long-term survival after liver transplantation. *American Journal of Transplantation* 12(8):2181–2187.
- Morrisett, J.D., Abdel-Fattah, G., Kahan, B.D., 2003. Sirolimus changes lipid concentrations and lipoprotein metabolism in kidney transplant recipients. *Transplantation Proceedings* 35(3 Suppl):143S–150S.
- Sarbasov, D.D., Ali, S.M., Sengupta, S., Sheen, J.H., Hsu, P.P., Bagley, A.F., et al., 2006. Prolonged rapamycin treatment inhibits mTORC2 assembly and Akt/PKB. *Molecular Cell* 22(2):159–168.
- Schreiber, K.H., Ortiz, D., Academia, E.C., Anies, A.C., Liao, C.Y., Kennedy, B.K., 2015. Rapamycin-mediated mTORC2 inhibition is determined by the relative expression of FK506-binding proteins. *Aging Cell* 14(2):265–273.
- Lamming, D.W., Ye, L., Katajisto, P., Goncalves, M.D., Saitoh, M., Stevens, D.M., et al., 2012. Rapamycin-induced insulin resistance is mediated by mTORC2 loss and uncoupled from longevity. *Science* 335(6076):1638–1643.
- Kennedy, B.K., Lamming, D.W., 2016. The mechanistic target of rapamycin: the grand Conductor of metabolism and aging. *Cell Metabolism* 23(6):990–1003.
- Chakrabarti, P., Kim, J.Y., Singh, M., Shin, Y.K., Kim, J., Kumbriak, J., et al., 2013. Insulin inhibits lipolysis in adipocytes via the evolutionarily conserved mTORC1-Egr1-ATGL-mediated pathway. *Molecular and Cellular Biology* 33(18):3659–3666.
- Kraemer, F.B., Takeda, D., Natu, V., Sztalryd, C., 1998. Insulin regulates lipoprotein lipase activity in rat adipose cells via wortmannin- and rapamycin-sensitive pathways. *Metabolism* 47(5):555–559.
- Houde, V.P., Brule, S., Festuccia, W.T., Blanchard, P.G., Bellmann, K., Deshaies, Y., et al., 2010. Chronic rapamycin treatment causes glucose intolerance and hyperlipidemia by upregulating hepatic gluconeogenesis and impairing lipid deposition in adipose tissue. *Diabetes* 59(6):1338–1348.
- Hagiwara, A., Cornu, M., Cybulski, N., Polak, P., Betz, C., Trapani, F., et al., 2012. Hepatic mTORC2 activates glycolysis and lipogenesis through Akt, glucokinase, and SREBP1c. *Cell Metabolism* 15(5):725–738.
- Soliman, G.A., Acosta-Jaquez, H.A., Fingar, D.C., 2010. mTORC1 inhibition via rapamycin promotes triacylglycerol lipolysis and release of free fatty acids in 3T3-L1 adipocytes. *Lipids* 45(12):1089–1100.
- Yecies, J.L., Zhang, H.H., Menon, S., Liu, S., Yecies, D., Lipovsky, A.I., et al., 2011. Akt stimulates hepatic SREBP1c and lipogenesis through parallel mTORC1-dependent and independent pathways. *Cell Metabolism* 14(1):21–32.
- Yuan, M., Pino, E., Wu, L., Kacergis, M., Soukas, A.A., 2012. Identification of Akt-independent regulation of hepatic lipogenesis by mammalian target of rapamycin (mTOR) complex 2. *Journal of Biological Chemistry* 287(35):29579–29588.
- Tory, R., Sachs-Barrable, K., Hill, J.S., Wasan, K.M., 2008. Cyclosporine A and Rapamycin induce in vitro cholesteryl ester transfer protein activity, and suppress lipoprotein lipase activity in human plasma. *International Journal of Pharmaceutics* 358(1–2):219–223.
- Peterson, T.R., Sengupta, S.S., Harris, T.E., Carmack, A.E., Kang, S.A., Balderas, E., et al., 2011. mTOR complex 1 regulates lipin 1 localization to control the SREBP pathway. *Cell* 146(3):408–420.
- Quinn 3rd, W.J., Wan, M., Shewale, S.V., Gelfer, R., Rader, D.J., Birnbaum, M.J., et al., 2017. mTORC1 stimulates phosphatidylcholine synthesis to promote triglyceride secretion. *Journal of Clinical Investigation* 127(11):4207–4215.
- Chakrabarti, P., English, T., Shi, J., Smas, C.M., Kandror, K.V., 2010. Mammalian target of rapamycin complex 1 suppresses lipolysis, stimulates lipogenesis, and promotes fat storage. *Diabetes* 59(4):775–781.
- Blanchard, P.G., Festuccia, W.T., Houde, V.P., St-Pierre, P., Brule, S., Turcotte, V., et al., 2012. Major involvement of mTOR in the PPARgamma-induced stimulation of adipose tissue lipid uptake and fat accretion. *The Journal of Lipid Research* 53(6):1117–1125.
- Fang, Y., Westbrook, R., Hill, C., Boparai, R.K., Arum, O., Spong, A., et al., 2013. Duration of rapamycin treatment has differential effects on metabolism in mice. *Cell Metabolism* 17(3):456–462.
- Fang, Y., Hill, C.M., Darcy, J., Reyes-Ordóñez, A., Arauz, E., McFadden, S., et al., 2018. Effects of rapamycin on growth hormone receptor knockout mice. *Proceedings of the National Academy of Sciences of the United States of America*. *Metabolism* 115(7):E1495–E1503.
- Lopes, P.C., Fuhrmann, A., Sereno, J., Espinoza, D.O., Pereira, M.J., Eriksson, J.W., et al., 2014. Short and long term in vivo effects of Cyclosporine A and Sirolimus on genes and proteins involved in lipid metabolism in Wistar rats. *Metabolism* 63(5):702–715.
- Pereira, M.J., Palming, J., Rizell, M., Aureliano, M., Carvalho, E., Svensson, M.K., et al., 2013. The immunosuppressive agents rapamycin, cyclosporin A and tacrolimus increase lipolysis, inhibit lipid storage and alter expression of genes involved in lipid metabolism in human adipose tissue. *Molecular and Cellular Endocrinology* 365(2):260–269.
- Polak, P., Cybulski, N., Feige, J.N., Auwerx, J., Ruegg, M.A., Hall, M.N., 2008. Adipose-specific knockout of raptor results in lean mice with enhanced mitochondrial respiration. *Cell Metabolism* 8(5):399–410.
- Lee, K.Y., Russell, S.J., Ussar, S., Boucher, J., Vernochet, C., Mori, M.A., et al., 2013. Lessons on conditional gene targeting in mouse adipose tissue. *Diabetes* 62(3):864–874.
- Tran, C.M., Mukherjee, S., Ye, L., Frederick, D.W., Kissig, M., Davis, J.G., et al., 2016. Rapamycin blocks induction of the thermogenic program in white adipose tissue. *Diabetes* 65(4):927–941.
- Lee, P.L., Tang, Y., Li, H., Guertin, D.A., 2016. Raptor/mTORC1 loss in adipocytes causes progressive lipodystrophy and fatty liver disease. *Molecular Metabolism* 5(6):422–432.

- [31] Eguchi, J., Wang, X., Yu, S., Kershaw, E.E., Chiu, P.C., Dushay, J., et al., 2011. Transcriptional control of adipose lipid handling by IRF4. *Cell Metabolism* 13(3):249–259.
- [32] Sengupta, S., Peterson, T.R., Laplante, M., Oh, S., Sabatini, D.M., 2010. mTORC1 controls fasting-induced ketogenesis and its modulation by ageing. *Nature* 468(7327):1100–1104.
- [33] Sitnick, M.T., Basantani, M.K., Cai, L., Schoiswohl, G., Yazbeck, C.F., Distefano, G., et al., 2013. Skeletal muscle triacylglycerol hydrolysis does not influence metabolic complications of obesity. *Diabetes* 62(10):3350–3361.
- [34] Papazyan, R., Sun, Z., Kim, Y.H., Titchenell, P.M., Hill, D.A., Lu, W., et al., 2016. Physiological suppression of lipotoxic liver damage by complementary actions of HDAC3 and SCAP/SREBP. *Cell Metabolism* 24(6):863–874.
- [35] Melamud, E., Vastag, L., Rabinowitz, J.D., 2010. Metabolomic analysis and visualization engine for LC-MS data. *Analytical Chemistry* 82(23):9818–9826.
- [36] Huang, J., Manning, B.D., 2009. A complex interplay between Akt, TSC2 and the two mTOR complexes. *Biochemical Society Transactions* 37(Pt 1):217–222.
- [37] Saxena, U., Witte, L.D., Goldberg, I.J., 1989. Release of endothelial cell lipoprotein lipase by plasma lipoproteins and free fatty acids. *Journal of Biological Chemistry* 264(8):4349–4355.
- [38] Amri, E.Z., Teboul, L., Vannier, C., Grimaldi, P.A., Ailhaud, G., 1996. Fatty acids regulate the expression of lipoprotein lipase gene and activity in preadipose and adipose cells. *Biochemical Journal* 314(Pt 2):541–546.
- [39] Bengtsson, G., Olivecrona, T., 1980. Lipoprotein lipase. Mechanism of product inhibition. *European Journal of Biochemistry* 106(2):557–562.
- [40] Sakurai, T., Davenport, R., Stafford, S., Grosse, J., Ogawa, K., Cameron, J., et al., 2014. Identification of a novel GPR81-selective agonist that suppresses lipolysis in mice without cutaneous flushing. *European Journal of Pharmacology* 727:1–7.
- [41] Ge, H., Weiszmann, J., Reagan, J.D., Gupte, J., Baribault, H., Gyuris, T., et al., 2008. Elucidation of signaling and functional activities of an orphan GPCR, GPR81. *The Journal of Lipid Research* 49(4):797–803.
- [42] Kim, J.E., Chen, J., 2004. Regulation of peroxisome proliferator-activated receptor-gamma activity by mammalian target of rapamycin and amino acids in adipogenesis. *Diabetes* 53(11):2748–2756.
- [43] Chatterjee, R., Bhattacharya, P., Gavrilova, O., Glass, K., Moitra, J., Myakishev, M., et al., 2011. Suppression of the C/EBP family of transcription factors in adipose tissue causes lipodystrophy. *Journal of Molecular Endocrinology* 46(3):175–192.
- [44] Tansey, J.T., Sztalryd, C., Gruia-Gray, J., Roush, D.L., Zee, J.V., Gavrilova, O., et al., 2001. Perilipin ablation results in a lean mouse with aberrant adipocyte lipolysis, enhanced leptin production, and resistance to diet-induced obesity. *Proceedings of the National Academy of Sciences of the United States of America* 98(11):6494–6499.
- [45] Koster, A., Chao, Y.B., Mosior, M., Ford, A., Gonzalez-DeWhitt, P.A., Hale, J.E., et al., 2005. Transgenic angiotensin-like (angptl)4 overexpression and targeted disruption of angptl4 and angptl3: regulation of triglyceride metabolism. *Endocrinology* 146(11):4943–4950.
- [46] Sukonina, V., Lookene, A., Olivecrona, T., Olivecrona, G., 2006. Angiotensin-like protein 4 converts lipoprotein lipase to inactive monomers and modulates lipase activity in adipose tissue. *Proceedings of the National Academy of Sciences of the United States of America* 103(46):17450–17455.
- [47] Gordts, P.L., Nock, R., Son, N.H., Ramms, B., Lew, I., Gonzales, J.C., et al., 2016. ApoC-III inhibits clearance of triglyceride-rich lipoproteins through LDL family receptors. *Journal of Clinical Investigation* 126(8):2855–2866.
- [48] Peterson, J., Bihain, B.E., Bengtsson-Olivecrona, G., Deckelbaum, R.J., Carpentier, Y.A., Olivecrona, T., 1990. Fatty acid control of lipoprotein lipase: a link between energy metabolism and lipid transport. *Proceedings of the National Academy of Sciences of the United States of America* 87(3):909–913.
- [49] Montserrat-de la Paz, S., Lopez, S., Bermudez, B., Guerrero, J.M., Abia, R., Muriana, F.J., 2018. Effects of immediate-release niacin and dietary fatty acids on acute insulin and lipid status in individuals with metabolic syndrome. *Journal of the Science of Food and Agriculture* 98(6):2194–2200.
- [50] Usman, M.H., Qamar, A., Gadi, R., Lilly, S., Goel, H., Hampson, J., et al., 2012. Extended-release niacin acutely suppresses postprandial triglyceridemia. *American Journal of Medicine* 125(10):1026–1035.
- [51] Kumar, A., Lawrence Jr., J.C., Jung, D.Y., Ko, H.J., Keller, S.R., Kim, J.K., et al., 2010. Fat cell-specific ablation of rictor in mice impairs insulin-regulated fat cell and whole-body glucose and lipid metabolism. *Diabetes* 59(6):1397–1406.
- [52] Schreiber, K.H., Arriola Apelo, S.I., Yu, D., Brinkman, J.A., Velarde, M.C., Syed, F.A., et al., 2019. A novel rapamycin analog is highly selective for mTORC1 in vivo. *Nature Communications* 10(1):3194.